Experimental observation of the rotation properties of atomic multipoles

Dieter Suter and Thomas Marty

Institute of Quantum Electronics, Swiss Federal Institute of Technology (ETH) Zürich, CH-8093 Zürich, Switzerland

Received April 20, 1993; revised manuscript received July 13, 1993

The resonant interaction of optical radiation with atomic vapors can excite the atoms into anisotropic states with long lifetimes. The conventional description of these states uses an expansion in a basis of multipole moments, which are represented by irreducible tensor operators. We demonstrate an experimental method that permits the excitation of these atomic multipole moments in specific, experimentally controllable spatial orientations. Complementary optical methods permit the observation of multipole moments of arbitrary order and a direct measurement of their spatial orientation. We demonstrate these procedures in the ground state of atomic sodium, using optical pumping to polarize the angular-momentum substates. We show how the experimental results can be used to separate signal contributions that originate from different multipole moments.

1. INTRODUCTION

Resonant interaction with polarized light converts atomic vapors from the homogeneous, isotropic thermal equilibrium to a state that is inherently anisotropic. The conventional description expands these states in a basis of multipole moments or, in mathematical terminology, in irreducible tensor components.[1] The first terms of this expansion, the magnetic dipole and electric quadrupole moments, are well known to affect various linear and especially nonlinear magneto-optical effects.[2-7] Because of their long lifetimes, multipole moments in the electronic ground state appear at the lowest intensities and cause the highest optical nonlinearities. These states can be prepared conveniently with optical pumping.[1,8-10] In a magnetic field parallel to the direction of the laser beam, or in zero magnetic field, optical pumping excites atomic states with rotational symmetry around the direction of the laser beam; in a multipole expansion of these atomic states, only terms of order $q = 0$ appear. If the rotational symmetry is broken, e.g., by a magnetic field perpendicular to the laser beam,[11,12] this selection rule is annulled, and in general it is possible for all multipole components to be excited also. In a quantum-mechanical description, terms with $q \neq 0$ correspond to coherent superpositions of different angular-momentum eigenstates.

Several of these sublevel coherences contribute to the anisotropic complex susceptibility of the medium and can therefore be observed optically[13-16] in a process that may also be considered a resonant stimulated Raman process.[17,18] The resonance frequencies are determined by the splittings between those ground-state sublevels whose coherent superposition corresponds to the multipole moments. Using spectroscopic information from experiments of this type, it is possible for one to study, e.g., the polarizability[19] and the relaxation[20-22] of atomic multipoles. The long lifetime of ground-state multipole moments[23] makes it possible for significant polarization of these sublevel multiplets to be achieved, even at very low laser intensities ($I < 1\ \mu\text{m mm}^{-2}$). For the same reason, the natural width of the Raman resonances is in general very small (<1 Hz), and the observed linewidths are independent of the width of the optical transition and the laser linewidth. Under optimized experimental conditions the observed linewidths can fall into the subhertz range.[24]

Direct optical observation of atomic multipole moments is possible and has been reported for dipole moments[13,15,16,25] and quadrupole moments.[14,16,26,27] Higher moments are not accessible in direct optical experiments,[16,28] but indirect evidence has been obtained for moments as high as hexadecupole moments.[3,4] The methods used for such observations are either zero-field level-crossing experiments[3,4] or Raman-type experiments in a static magnetic field.[13,15,16,25] These types of experiment have the advantage that the signal contributions are spread out in the frequency dimension, and the precession frequency may help to identify the different multipole moments. Even so, a complete characterization of such an anisotropic atomic state may be rather demanding, especially in systems with nonvanishing nuclear spin: an atomic state with total angular momentum F must be expanded in terms of irreducible tensor operators of rank $0 \leq k \leq 2F$ with a total of $(2F + 1)^2$ components. A complete characterization of the atomic state requires, therefore, the measurement of $(2F + 1)^2$ independent variables.

The first obstacle that must be overcome before a complete characterization of such atomic states is feasible is the selection rule that prevents direct optical observation of multipole moments with order $q > 2$. Higher-order moments cannot affect the optical properties of the medium, since the relevant processes would involve the exchange of more than two quanta of angular momentum between the atomic system and the photons. Their detection in optical experiments therefore requires a multistep process. We recently demonstrated such a procedure, which permits the observation of all multi-

0740-3224/94/010242-11$06.00

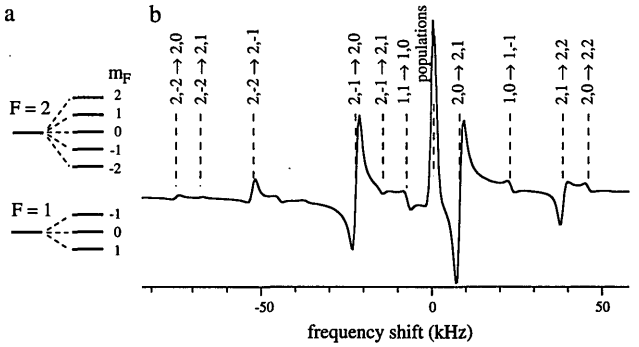

Fig. 1. a, Energy-level system of the sodium ground state and b, calculated sublevel spectrum in a magnetic field of 0.7 mG. The numbers above the resonance lines indicate the assignment to the sublevel transitions in the form $(F, m_F \leftrightarrow F', m_{F'})$. The origin of the frequency axis is at 5.2 MHz.

pole moments.[29] It uses a laser-induced transfer of sublevel coherence from the forbidden higher moments to a sublevel transition that can be observed directly. This technique permits the observation of the different multipole components not only in a static manner but also as they evolve as a function of time. Fourier transformation of the time-domain data yields a spectrum of the sublevel transitions in which the various multipole moments appear as individual resonance lines.

In such a spectrum of an atomic system with nonvanishing nuclear spin, the large number of resonances increases the likelihood of overlap between the resonance lines. Figure 1 illustrates this problem with an example from the ground state of atomic sodium. The left-hand part shows the relevant energy-level scheme, while the right-hand part represents the calculated sublevel spectrum as it could be observed with the technique described in Ref. 29. The numbers above the resonances show the assignment to the sublevel transitions in the form $(F, m_F \leftrightarrow F', m_{F'})$. In crowded spectra overlap between different resonance lines can make it impossible for the signal contributions to be separated and can prevent an assignment to the sublevel transitions. This problem is already evident in this calculated spectrum; in experimental data the finite resolution and signal-to-noise ratios aggravate the problem even further. In those cases additional means for characterizing signal contributions are often helpful.

In this paper we demonstrate a possible method for characterizing signal contributions from different atomic multipole moments. The method directly uses the rotational transformation properties of irreducible tensor operators: in a sequence of experiments, laser pulses excite the atomic system into states that differ by a rotation around the symmetry axis of the system. For the irreducible components of the ground-state density operator, this rotation corresponds by definition to a multiplication with a phase factor $\exp(iq\phi)$, whose phase is given by the rotation angle ϕ and the tensorial order q. This signal phase can be observed as a change of the line shape in the sublevel spectrum. By comparing the line shapes among the different experiments, it is therefore possible to distinguish contributions from different atomic multipole moments and to measure their orientation in space.[30]

The paper is structured as follows: in the following section we present the principle of the method without technical details; this should allow the reader to grasp the idea of the technique without having to plow through the mathematical formalism, which we use in Section 3 for a more thorough theoretical description of the system and the relevant dynamics. Section 4 describes the experimental realization and presents a comparison of experimental data with theoretical predictions. In the concluding section we summarize the results and discuss additional possibilities.

2. PRINCIPLE AND OVERVIEW

A. System

As is discussed above, we are interested primarily in atomic multipole moments of the electronic ground state. As a particular example, we choose the $3s\,^2S_{1/2}$ ground state of atomic sodium and use the D_1 resonance line as the optical transition that couples to the laser field. The level scheme of the sodium ground state is represented schematically in Fig. 1. The electronic spin of $S = 1/2$ and the nuclear spin of $I = 3/2$ couple through the hyperfine interaction, which splits the angular-momentum substates into two multiplets with total angular momentum $F = 1, 2$. In the theoretical and the experimental sections, we concentrate on the $F = 2$ multiplet, for which multipole moments as high as the hexadecupole (rank $k = 4$) are possible. We consider only the case in which the Zeeman interaction, and therefore the energy-level separation within the $F = 2$ multiplet, is small compared with the hyperfine splitting.

The experiment that we discuss here belongs to the pump-and-probe category. As is shown schematically in Fig. 2, a circularly polarized pump laser beam excites the multipole moments in the medium, where they evolve under the influence of magnetic fields and the interaction with the pump laser. A second laser beam serves as the probe beam: the presence of the multipole moments makes the atomic medium birefringent as well as dichroic, i.e., its refractive index, as well as its absorption coefficient, depends on the polarization of the light. The polarization of the probe beam changes, therefore, as it propagates through the medium in a manner that depends on the optical anisotropy of the medium. Behind the sample cell a polarization-selective detector converts these polarization changes into the observed signal, which is therefore a measure of the multipole moments present in the system. The intensity of this probe laser beam should be low enough that it does not significantly affect the dynamics of the system.

This separation of the interaction between the atomic medium and the laser field into pumping and probing

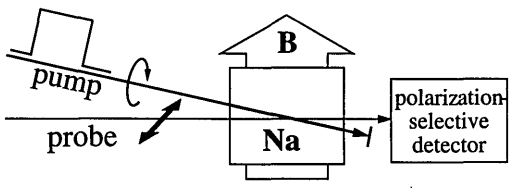

Fig. 2. Principle of the pump–probe experiment used to create and observe atomic multipole moments. B, Magnetic field.

processes is also reflected in the theoretical analysis: we discuss primarily the evolution of the system and consider the probe beam only in the sense that we calculate expectation values, which are proportional to the signal obtained from the probe laser beam, but neglect its influence on the dynamics of the system. The pump laser beam can be switched on and off electronically; in the experiment we use this feature for preparing the atomic multipole moments with a pump laser pulse and subsequently switch the pump pulse off to observe the system during free evolution.

B. Time-Domain Spectroscopy

One can distinguish atomic multipole moments perpendicular to the magnetic field by monitoring their precession.[13,15,16,25] This possibility is derived directly from the definition of irreducible tensor operators: a tensor component of order q is invariant under rotations by $2\pi/q$. When the system undergoes Larmor precession in an external magnetic field, the signal contributions that are due to those tensor components must be periodic with period $2\pi/(q\Omega_L)$, $1/q$ times the Larmor period. Time-dependent signal contributions from different tensor components can therefore be separated by Fourier analysis of the signal.

Excitation of the multipole moments in a transverse magnetic field has to compete with the Larmor precession and therefore leads, for constant optical pumping, to only small anisotropies. However, modulating the optical pumping at a frequency close to the Larmor frequency permits efficient excitation of precessing atomic multipoles.[11] The excitation of multipole moments in these experiments is clearly a resonant process. One can ensure that resonance condition is fulfilled either by scanning the modulation frequency in a constant magnetic field or by keeping the modulation frequency constant while sweeping the magnetic field. The resonance frequency contains the information about the order of the multipole moment as well as the strength of the Zeeman interaction.

Time-domain experiments can provide the same information by simultaneous excitation of a number of multipole moments and observation of their Larmor precession as a function of time.[13,23,25,31] The resulting Raman beat or free-induction-decay signal can then be Fourier transformed and converted into a sublevel spectrum that contains the same information as the one obtained in the slow-passage or continuous-wave (cw) experiment.[32] As we show below, this method of time-domian spectroscopy is more flexible than the cw method; in particular, it can be extended to the observation of higher-order moments that are not accessible with cw experiments.

In a typical time-resolved experiment a polarized laser pulse excites the system by optical pumping in a constant magnetic field. In a transverse magnetic field such a laser pulse in general excites all possible multipole moments. In close analogy to the cw experiments, the probe laser beam measures the circular birefringence of the medium, which is proportional to the component of the magnetic dipole moment in the direction of the laser beam. If the magnetic dipole moment undergoes Larmor precession, the signal is modulated at the Larmor frequency; Fourier transformation of time-dependent signal yields a spectrum containing a resonance line at the Larmor frequency. The lifetime of the magnetic dipole determines the widths of the resonance lines in the resulting sublevel spectrum.

Figure 3 shows the procedure and an example from the sodium ground state. The uppermost trace indicates the amplitude of the pump laser beam as a function of time. The second trace shows the system response, measured by polarization-selective detection of a transmitted probe beam. The signal is proportional to the magnetic dipole component in the direction of the laser beam. During the pulse the laser light polarizes the electronic ground state, which evolves from the isotropic equilibrium state toward a new equilibrium state with a macroscopic magnetic dipole moment. After the end of the pulse the system undergoes Larmor precession in a transverse magnetic field. In this example the ground-state sublevels are not equidistant. Coherences between different ground-state sublevels therefore evolve at different frequencies, and the interference between them results in the beat pattern that is observed after the laser pulse. The third trace shows the corresponding sublevel spectrum, which was obtained by Fourier transformation of the free-precession signal. The individual resonances can be assigned to different transitions among angular-momentum substates. All signal contributions observed here arise from coherences between angular-momentum substates whose magnetic quantum numbers differ by ± 1.

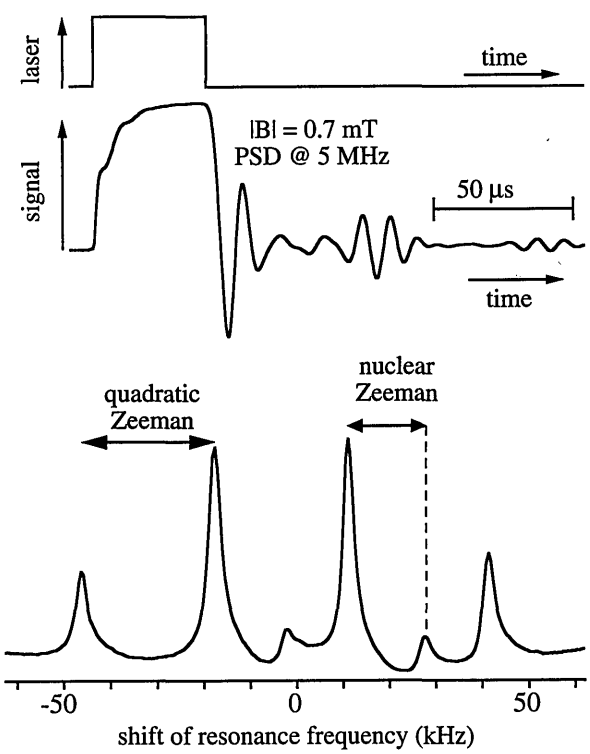

Fig. 3. Example of time-domain sublevel spectroscopy. The top trace shows the time dependence of the pump laser intensity. The second trace represents the signal recorded by polarization-selective detection of the transmitted probe beam. The bottom trace contains the sublevel spectrum, which was obtained by Fourier transformation and contains signal contributions from $q = \pm 1$ multipole moments. B, Magnetic field strength; PSD, phase-sensitive detection.

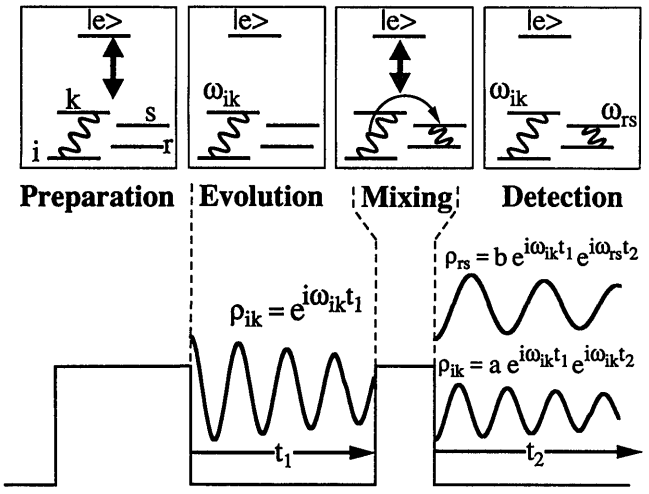

Fig. 4. Principle of two-dimensional time-resolved spectroscopy. The insets indicate the evolution of the system. The bottom trace corresponds to the pump laser intensity as a function of time.

C. Indirect Detection

The laser pulse in general excites not only a magnetic dipole moment but also various higher-order moments. However, multipole moments with orders higher than 2 (in general) or 1 (in the present system) do not affect the linear optical properties of the medium. Therefore the conventional observation of the system with a probe laser beam cannot detect the presence of these higher-order multipoles. A possible way around this limitation relies on laser-induced coherence transfer of the invisible multipole moments into observable sublevel coherences.[29,33] The procedure is closely related to two-dimensional spectroscopy, a technique that was first proposed by Jeener[34,35] and is now widely used in magnetic resonance spectroscopy,[36] while applications to optical spectroscopy have been demonstrated only recently.[29,37]

Figure 4 outlines the principle of the method. A first laser pulse couples to the electronic transition and excites, in a Raman-type process, a nonequilibrium state in the electronic ground state. The atomic multipole moments correspond to coherences among different angular momentum substates. The wavy line between substates i and k represents an example of such a coherence. After the end of the preparation pulse, these multipole moments precess freely for a time t_1 under the influence of the Zeeman interaction. The spectroscopic information is contained in the phase factors $\exp(i\omega_{ik}t_1)$, which the coherence acquires during this precession period. In the case of higher-order multipole moments, it is not possible to observe this phase information directly.

Instead a second laser pulse transfers this phase information to an observable sublevel transition. This laser-induced exchange process occurs during the period labeled Mixing in Fig. 4. It transfers the phase information to a density-operator element $\rho_{rs}(t_2)$, which is then proportional to the phase factor $\exp(i\omega_{ik}t_1)$. By measuring this phase factor and repeating the experiment for a number of t_1 values, it is possible to trace out the free precession of the coherence in the sublevel transition ρ_{ik}. Such a sequence of experiments is essentially equivalent to data observed for the dipole moment in the free-induction decay following a single excitation pulse. With this experimental procedure it is possible to observe not only multipole moments that change the optical properties of the system but also those that can be converted to directly observable moments by a laser pulse. The sensitivity for the different elements depends on the efficiency of the transfer process through various experimental parameters, such as the intensity and wavelength of the laser or the duration of the mixing pulse.

During the direct as well as during the indirect observation, the precession of the multipole moments is observed experimentally as an oscillation. Its instantaneous orientation therefore appears as the phase of the signal. If only a single multipole moment contributes to the signal, it is therefore possible to infer its instantaneous orientation at a given time from the observed data, as shown in Fig. 5. The upper part of the figure shows the precession of a magnetic dipole moment: the curve represents the observed signal, while the insets indicate the orientation of the dipole moment at various instances. The lower trace shows the same for a second-order tensor. The precession frequency is the same as for the dipole, but a 90° rotation of this multipole moment corresponds to a multiplication with -1, and a 180° rotation turns it into a state that is indistinguishable from the initial state. The observed signal therefore oscillates at twice the Larmor frequency. The signal frequency is a gauge for the order of the multipole moment, while the signal phase is a measure of its instantaneous orientation. Both the signal frequency and the phase as a function of the orientation can therefore be used to distinguish signal contributions from different multipole moments.

D. Modulation and Rotating Frame

Optical pumping in transverse magnetic fields must compete with the Zeeman effect: the Larmor precession spreads the order that the optical pumping

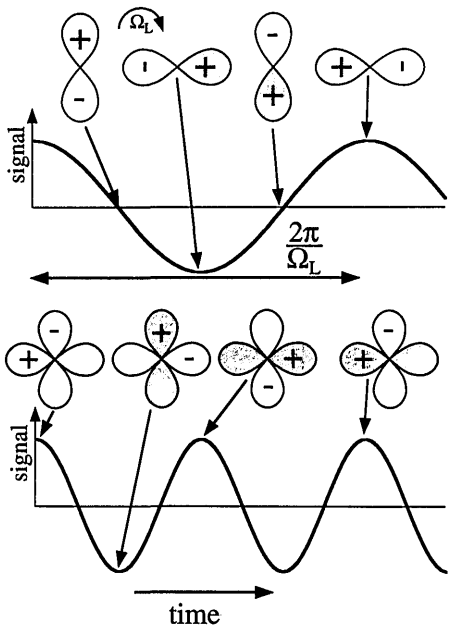

Fig. 5. Larmor precession of multipoles and observable signal for dipoles (upper part) and second-order tensor elements (lower part).

process creates in the plane perpendicular to the magnetic field, leading to destructive interference. This process can be countered by modulation of the optical pumping rate.[11,38,39] This modulation resonantly enhances the optical pumping efficiency when the modulation frequency matches the Larmor frequency of the system. The effect can be explained easily if the dynamics of the system are described in a coordinate system that rotates around the direction of the magnetic field at the modulation frequency. In this reference frame the evolution of the system can be described by a time-independent effective Hamiltonian and a time-independent optical pumping rate.

The Hamiltonian and the optical pumping process in this reference frame also depend on the phase of the modulation. If the other parameters remain unchanged, a shift of the modulation phase corresponds to a rotation of the rotating-frame Hamiltonian. This phase dependence makes it possible for one to control the orientation of the atomic multipoles simply by adjusting the phase of a radio-frequency signal. We use this method to excite the atomic system into states that differ only by a rotation around the direction of the magnetic field. This rotation of the atomic state corresponds quantum mechanically to a multiplication of the individual multipole moments by a phase factor that is proportional to the order of the component. Signal components resulting from these multipole components are of course multiplied by the same phase factors. The measurement of the signal phase for different atomic states therefore permits the determination of the orientation of the individual components as well as the assignment of signal components to specific multipoles.

3. THEORY

A. System and Hamiltonian

While the principle of this technique is completely general, we use a specific system to illustrate the procedure. For our example, we choose the $3s\,^2S_{1/2}$ ground state of atomic sodium. The electronic angular momentum of $J = 1/2$ in this state couples to the nuclear spin $I = 3/2$; the angular-momentum states therefore group into two hyperfine multiplets with total angular momentum $F = 1, 2$. Distinguishing among various multipole moments is of particular interest when their lifetimes are long. Under the experimental conditions that we consider here, atomic diffusion limits the observation times. The experimentally observed effective lifetimes are of the order of 1 ms. If the laser intensities are well below the saturation level of the electronic transition, the excited-state populations are small, and the optical properties of the system are determined by the electronic ground state alone. The system that we consider in our calculation therefore consists of only the eight sublevels of the electronic ground state.

The relevant Hamiltonian for this system can be written as

$$\mathcal{H}_g = A\mathbf{J}\cdot\mathbf{I} - \mu_J\mathbf{B}\cdot\mathbf{J} - \mu_I\mathbf{B}\cdot\mathbf{I} \tag{1}$$

in units for which $\hbar = 1$. A represents the hyperfine coupling constant, μ_J and μ_I the Zeeman coupling constants, $\mathbf{J} = (J_x, J_y, J_z)$ the electronic angular-momentum operator, $\mathbf{I} = (I_x, I_y, I_z)$ the nuclear spin operator, and $\mathbf{B} = (B_x, B_y, B_z)$ the magnetic field. In the context of this paper we make an additional simplification and consider only the $F = 2$ multiplet of the electronic ground state. For the relatively weak magnetic fields in which we are interested it is possible to use the Breit–Rabi low-field approximation of the Hamiltonian, which is valid as long as the Zeeman interaction is small compared with the hyperfine splitting:

$$\mathcal{H}_2 = -\mu_F B F_z - \mu_F^{(2)} B^2 {F_z}^2, \tag{2}$$

where we have chosen the z axis parallel to the magnetic-field direction. μ_F and $\mu_F^{(2)}$ are the Zeeman coupling constants for the linear and the quadratic Zeeman interaction; the numerical values for the sodium ground state are $\mu_F = 7$ MHz/mT and $\mu_F^{(2)} = 27$ kHz mT^{-2}. The Hamiltonian of Eq. (2) is symmetric with respect to rotation around the z axis. It is therefore convenient for us to express the density operator in a representation that transforms irreducibly under rotations around this axis, i.e., to expand it in terms of irreducible tensor operators $T_q^{(k)}$ of rank k and order q.[1] The ground-state density operator then becomes

$$\rho = \sum_{kq} a_{kq} T_q^{(k)}, \tag{3}$$

with a_{kq} representing the expansion coefficients. The evolution of the density operator under the Zeeman interaction is

$$\rho(t) = \exp(i\mu_F^{(2)} B^2 t {F_z}^2)\exp(i\Omega_L t F_z)\rho(0) \times \exp(-i\Omega_L t F_z)\exp(-i\mu_F^{(2)} B^2 t {F_z}^2). \tag{4}$$

Here we have separated the Zeeman effect into a term linear in the field, describing the Larmor precession at frequency $\Omega_L = \mu_F B$, and a term quadratic in the field. Like every rotation around the symmetry axis, the Larmor precession leads only to a phase accumulation of the individual tensorial components:

$$\rho(t) = \exp(i\mu_F^{(2)} B^2 t {F_z}^2)\left[\sum_{kq}\exp(-iq\Omega_L t)a_{kq}T_q^{(k)}\right] \times \exp(-i\mu_F^{(2)} B^2 t {F_z}^2). \tag{5}$$

The quadratic Zeeman effect also conserves the order q of the tensor operators, but not their rank k, indicating that it cannot be described as a rotation in three-dimensional space. We therefore introduce, besides the irreducible tensor operators, another set of operators $A_{q,r}$, which transform irreducibly under rotations around the z axis as well as under the Hamiltonian evolution. These operators are linear combinations of irreducible tensor operators $T_q^{(k)}$ with the same order q:

$$A_{q,r} = \sum_{k=|q|}^{2F} \alpha_{kqr} T_q^{(k)}. \tag{6}$$

The transformation under rotations around the z axis therefore remains

$$\exp(-i\phi F_z)A_{q,r}\exp(i\phi F_z) = \exp(iq\phi)A_{q,r}, \tag{7}$$

and the Hamiltonian evolution is

$$\exp(-i\mathcal{H}t)A_{q,r}\exp(i\mathcal{H}t) = \exp(i\omega_{q,r}t)A_{q,r}. \tag{8}$$

In the eigenbase of the Hamiltonian, the operators $A_{q,r}$ have for $|q| > 0$ a single nonzero matrix element between two states whose magnetic quantum numbers differ by $m_F - m_{F'} = q$. The precession frequency $\omega_{q,r}$ of the operator $A_{q,r}$ is

$$\omega_{q,r} = q\Omega_L + \mu_F^{(2)} B^2 (m_F{}^2 - m_{F'}{}^2). \tag{9}$$

In this operator basis we expand the density operator as

$$\rho(0) = \sum_{q,r} d_{q,r} A_{q,r} \tag{10}$$

and write its time evolution as

$$\rho(t) = \sum_{q,r} \exp(i\omega_{q,r} t) d_{q,r} A_{q,r}. \tag{11}$$

When the pump laser drives the atomic system, additional effects contribute to the evolution. These laser-induced aspects of the dynamics[33,37] are not a central part of this paper, and we include them only in a qualitative manner: we use the fact that the interaction with laser radiation can excite and interchange multipole moments, and we discuss the possibilities for measuring their orientation and their behavior under rotations.

B. Rotating Frame

For experimental as well as for mathematical reasons it is often convenient to analyze the dynamics of the system not in the laboratory coordinate system but in a frame of reference rotating around the magnetic-field direction at an angular velocity close to the Larmor frequency. In this reference frame the Larmor precession is slower than in the laboratory system. Mathematically the transformation is expressed by the equations

$$\mathcal{H}^{(r)} = U\mathcal{H}U^\dagger - iUU^\dagger, \qquad \rho^{(r)} = U\rho U^\dagger, \tag{12}$$

where $\mathcal{H}^{(r)}$ and $\rho^{(r)}$ represent the Hamiltonian and the density operator in the rotating frame and the same quantities without the index refer to the laboratory coordinate system. The unitary transformation operator is

$$U = \exp(i\omega t F_z). \tag{13}$$

The rotating-frame Hamiltonian is therefore

$$\mathcal{H}_2^{(r)} = -(\Omega_L - \omega)F_z - \mu_F^{(2)} B^2 F_z{}^2, \tag{14}$$

and the rotating-frame density operator evolves as

$$\rho^{(r)}(t) = \sum_{q,r} \exp[i\omega_{q,r}^{(r)} t] d_{q,r} A_{q,r},$$

$$\omega_{q,r}^{(r)} = q(\Omega_L - \omega) + \mu_F^{(2)} B^2 (m_F{}^2 - m_{F'}{}^2). \tag{15}$$

In many experimental examples the Hamiltonian describing the coupling with the laser field in the laboratory frame includes time-dependent terms of the form

$$\mathcal{H}_{\text{mod}} = \exp(-i\omega_{\text{mod}} t F_z)\mathcal{H}_{\text{int}} \exp(i\omega_{\text{mod}} t F_z). \tag{16}$$

A straightforward application of Eqs. (12) and (13) shows that a transformation to a coordinate system rotating at ω_{mod} removes this time dependence, and the transformed operator is $\mathcal{H}_{\text{mod}}^{(r)} = \mathcal{H}_{\text{int}}$.[38]

Besides this time-dependent transformation, we come across time-independent rotations around the z axis. In an obvious analogy, we define operators that are rotated by an angle ϕ as

$$A(\phi) = \exp(-i\phi F_z) A(0) \exp(i\phi F_z). \tag{17}$$

The main interest in this transformation arises in the context of modulated Hamiltonians whose modulation phase ϕ can be controlled experimentally:

$$\mathcal{H}_{\text{mod}}(\phi) = \exp[-i(\omega_{\text{mod}} t + \phi)F_z]\mathcal{H}_{\text{int}} \times \exp[i(\omega_{\text{mod}} t + \phi)F_z]. \tag{18}$$

In the rotating frame this Hamiltonian becomes

$$\mathcal{H}_{\text{mod}}^{(r)}(\phi) = \exp(-i\phi F_z)\mathcal{H}_{\text{int}} \exp(i\phi F_z); \tag{19}$$

i.e., the shift of the modulation phase in the laboratory frame corresponds to a (time-independent) rotation in the rotating frame. If $\mathcal{H}_{\text{mod}}^{(r)}(\phi)$ excites the system into a state

$$\rho(t;\phi) = \exp[-\mathcal{H}_{\text{mod}}^{(r)}(\phi)t]\rho_{\text{eq}} \exp[\mathcal{H}_{\text{mod}}^{(r)}(\phi)t] = \exp(-i\phi F_z)\rho(t;\phi = 0)\exp(i\phi F_z), \tag{20}$$

starting from the isotropic thermal equilibrium state ρ_{eq}, the final atomic state $\rho(\phi)$ is rotated by the same angle compared with the state $\rho(0)$ prepared with the reference Hamiltonian with phase $\phi = 0$. We can therefore control the orientation of the atomic multipoles experimentally: Shifting the phase of the radio frequency by $\Delta\phi$ rotates the atomic state by an angle $\Delta\phi$.

C. Evolution and Detection

In a typical experiment the initial laser pulse excites the system into a state $\rho(0)$, where all (ground-state) density-operator elements are nonzero. The system is then allowed to precess freely under the influence of the magnetic field. With relaxation neglected, this evolution can be written as

$$\rho^{(r)}(t_1) = \exp[-i\mathcal{H}^{(r)}t_1]\rho_0 \exp[i\mathcal{H}^{(r)}t_1] = \sum_{q,r} d_{q,r} \exp[i\omega_{q,r}^{(r)} t_1] A_{q,r}. \tag{21}$$

In this and the following equations, the Hamiltonian and the density operator are expressed in the rotating coordinate system; however, for typographical clarity we now drop the index (r). The second pump laser pulse terminates the free-precession period and redistributes the coherence among the different multipole moments. We summarize its effect on the system formally by a matrix $R = (r_{q'r'qr})$,

$$\rho(t_1, 0) = \sum_{q',r'} A_{q',r'} \sum_{q,r} r_{q'r'qr} d_{q,r} \exp(i\omega_{qr} t_1). \tag{22}$$

After the second pulse the system is again allowed to precess freely as

$$\rho(t_1, t_2) = \sum_{q',r'} \exp(i\omega_{q'r'} t_2) A_{q',r'} \times \sum_{q,r} r_{q'r'qr} d_{q,r} \exp(i\omega_{qr} t_1). \tag{23}$$

The experimental setup measures the circular birefringence of the sample and produces a signal proportional to the expectation value of the magnetic dipole component

in the direction of the laser beam. In our experiment (see Fig. 7 below) we pass this signal through a phase-sensitive detector, selecting the positive frequency component that is proportional to the rotating-frame expectation value of

$$T_{-1}^{(1)} = \sum_{r=1}^{2F} b_{-1r} A_{-1r} . \tag{24}$$

The demodulated signal is therefore

$$\begin{aligned} S(t_1, t_2) &= \mathrm{Tr}[T_{-1}^{(1)} \rho(t_1, t_2)] \\ &= \sum_{r'} b_{-1r'} \exp(i\omega_{1r'} t_2) \sum_{q,r} r_{1r'qr} d_{q,r} \exp(i\omega_{qr} t_1) , \end{aligned} \tag{25}$$

where we have used the orthonormality of the A_{mk}, $\mathrm{Tr}[A_{q,r} A_{q',r'}] = \delta_{q,-q'} \delta_{r,r'}$. This expression lends itself to reinterpretation if we write it as

$$\begin{aligned} S(t_1) &= \sum_{q,r} c_{q,r} d_{q,r} \exp(i\omega_{qr} t_1) \\ &= \mathrm{Tr}[A_{\mathrm{eff}} \rho(t_1)] , \end{aligned} \tag{26}$$

where the numbers

$$c_{q,r} = \sum_{r'} b_{-1r'} \exp(i\omega_{1r'} t_2) r_{1r'qr} \tag{27}$$

represent the expansion coefficients of the effective observable

$$\begin{aligned} A_{\mathrm{eff}}(t_2) &= \sum_{q,r} c_{q,r} A_{-q,r} \\ &= \sum_{r'} b_{-1r'} \exp(i\omega_{1r'} t_2) \sum_{q,r} r_{1r'qr} A_{-q,r} . \end{aligned} \tag{28}$$

The operator $A_{\mathrm{eff}}(t_2)$ can be considered an effective observable for the time between the pulses. The expansion coefficients $c_{q,r}$ describe the sensitivity with which we can monitor the evolution of the multipole moments $A_{q,r}$; they depend on the matrix elements of R that describe the efficiency of the transfer of sublevel coherence by the mixing pulse. In general, all expansion coefficients $c_{q,r}$ are nonzero, and the signal $S(t_1)$ therefore contains contributions from all multipole moments. With the method outlined here it is thus possible to observe all density-operator elements, circumventing the selection rules that restrict the values of q appearing in the directly observable signal.

The sensitivity with which the individual components contribute to the signal, described by $c_{q,r}$, depends on t_2. It is therefore possible to choose a specific observable by measuring the system response at an arbitrary time t_2. In general, however, it is more convenient to record the signal as a function of the time t_2 after the second pulse and perform a Fourier transformation to get a sublevel spectrum as a function of the conjugate variable ω_2. This permits a separation of the individual terms contributing to the sum over r' in Eq. (27), if the corresponding resonance frequencies are nondegenerate. The effective observable is then

$$\begin{aligned} A_{\mathrm{eff}}(\omega_2) &= g(\omega_2) \sum_{q,r} r_{1r'qr} A_{-q,r} , \\ g(\omega_2) &= \mathcal{F}\left[\sum_{r'} b_{-1r'} \exp(i\omega_{1r'} t_2) \right] , \end{aligned} \tag{29}$$

where $g(\omega_2)$ describes the shape of the sublevel spectrum. With these effective observables, $A_{\mathrm{eff}}(\omega_2)$ or $A_{\mathrm{eff}}(t_2)$, it is possible to record a signal as a function of the precession time t_1, as shown by Eq. (26). The resulting signal can be Fourier transformed with respect to t_1 to yield a spectrum with resonance lines at positions ω_{qr} with complex amplitudes $c_{q,r} d_{q,r}$. An example of such a spectrum is shown in Fig. 1: it was calculated with parameters appropriate for the sodium ground state for the observable $A_{\mathrm{eff}}(t_2 = 0)$, i.e., by measurement of the signal immediately after the second pulse.

D. Rotations

As we have shown above, a shift of the modulation phase during the first pulse leads to a rotation of the effective Hamiltonian during the pulse and, if the system is in thermal equilibrium before the pulse, also to a rotation of the resulting atomic state. The rotated system subsequently evolves as

$$\begin{aligned} \rho(t_1; \phi) &= \exp(-i\phi F_z) \rho(t_1, 0) \exp(i\phi F_z) \\ &= \sum_{q,r} \exp(iq\phi) d_{q,r} \exp(i\omega_{qr} t_1) A_{q,r} . \end{aligned} \tag{30}$$

Obviously the density-operator components are now labeled with a phase $q\phi$, which is proportional to the tensorial order q. The same factor appears also in the observed signal

$$S(t_1, \phi) = \sum_{q,r} c_{q,r} d_{q,r} \exp(iq\phi) \exp(i\omega_{qr} t_1) . \tag{31}$$

Terms associated with a density-operator component of order q are phase shifted by $q\phi$ if a rotation by an angle ϕ is performed. This permits a direct determination of the tensorial order as well as the orientation of this multipole moment, if this phase factor can be observed experimentally.

The signal phase can most easily be measured in sublevel spectra of the type shown in Fig. 1, where the signal phase modifies the line shape. Figure 6 illustrates the observed line shape as a function of the signal phase for the case of a Lorentzian line shape. The left-hand column shows the real part of the complex line-shape

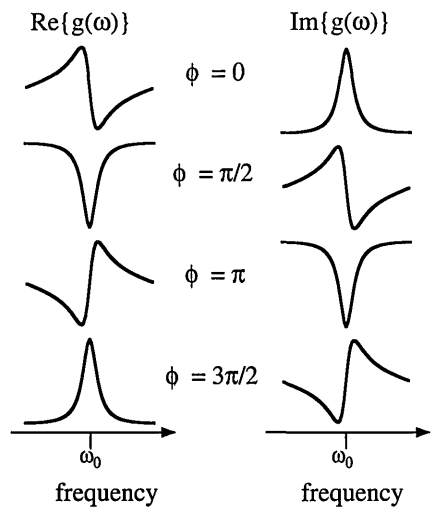

Fig. 6. Line shapes as functions of the signal phase for a complex Lorentzian line-shape function.

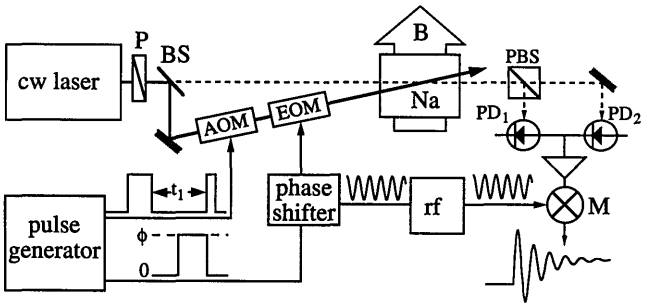

Fig. 7. Setup used for the experimental implementation. P, polarizer; BS, beam splitter, AOM, acousto-optic modulator; EOM, electro-optic modulator; rf, radio-frequency synthesizer; B, magnetic field; PBS, polarizing beam splitter; $PD_{1,2}$, photodiodes; M, mixer.

function, the right-hand column the imaginary part. If the phase changes by 90°, the line shape of the real part changes from dispersionlike to absorptionlike, and the imaginary part changes from an absorptive to a dispersive shape. A 180° phase shift inverts the signal, and intermediate phases lead to mixed phase lines. The actual signal phase can be recovered by line-shape analysis or by multiplication of the observed line shapes with an additional phase factor to transform the line shape into a pure absorption or dispersion line.

4. EXPERIMENTS

A. Setup

For the experimental implementation of the procedures described above, we used the setup shown schematically in Fig. 7. The atomic multipoles were created in the electronic ground state of atomic sodium. A 1-cm-long glass cell, heated to a temperature of 180 °C, contained the sodium vapor together with 200 mbars of argon. The collisions of the sodium atoms with the buffer gas cause a pressure broadening of the optical resonance line that masks the inhomogeneous Doppler broadening. The buffer gas also extends the lifetime of the ground-state multipole moments: they are relatively insensitive to collisions, and their effective lifetime is determined by the transit time of atoms through the laser beam. In the presence of the buffer gas, this motion is diffusive and much slower than under conditions of free flight. Under our experimental conditions the width of the pressure-broadened optical resonance line was 2.1 GHz half-width at half-maximum, and the lifetime of the ground-state multipole moments was close to 1 ms.

A single-mode cw ring dye laser with a short-term linewidth of less than 500 kHz produced the two laser beams. Their frequency was close to the sodium D_1 line ($\lambda = 589.6$ nm), with a detuning $\Delta = 12$ GHz above the center of the (pressure-shifted) resonance line, optimized for efficient detection of the invisible higher multipole moments with $|q| > 1$. The pump beam had an intensity of ~100 mW/mm^2; and the probe beam, ~100 μW/mm^2. The two beams overlapped in the sample region at an angle of less than 1°. A magnetic field of $B = 0.74$ mT was oriented perpendicular to the laser beams. An electro-optic crystal modulated the polarization of the pump laser beam between opposite circular polarizations. The modulation frequency of $\omega_m/2\pi = 5.2$ MHz was close to the Larmor frequency of the system. A computer-controlled digital delay generator controlled the timing of the experiment: it generated the laser pulses through acousto-optic modulator and shifted the phase of the radio-frequency applied to the electro-optic crystal, thereby controlling the orientation of the multipole moments in the sodium atoms.

After propagating through the vapor cell, the probe beam entered a polarization-selective detector[40,41] that measured the circular birefringence of the sample. The resulting signal was proportional to the ground-state magnetization component in the direction of the laser beam, i.e., perpendicular to the magnetic-field direction. In the laboratory coordinate system this component oscillates at the Larmor frequency. By the phase-sensitive detection indicated in the figure, we obtained a signal that corresponds to the evolution of the system in the rotating coordinate system.[38] This procedure reduces the speed requirements for the detection system significantly. After digitization, the data were transferred to the computer, where the corresponding sublevel spectra were calculated by Fourier transformation.

B. Orientation Dependence

To observe the orientation dependence of the multipole moments, we used the indirect detection scheme described in Subsection 3C. The time-domain data were Fourier transformed to separate the signal components from the different multipole moments. The orientation dependence of the signal components was measured by comparison of data sets obtained with different modulation phases during the first pulse, i.e., different orientation of the atomic multipole moments. During the second laser pulse we also modulated the polarization of the pump laser beam to effect an efficient coherence transfer, but this modulation phase was kept constant between experiments. For the experiments presented here the duration of the first pulse was set to 100 μs; the length of the second pulse was 2 μs.

Figure 8 shows some representative signal components from the observed spectra. As is explained above, we expect to see an effect of the phase shift on the different resonances that is proportional to the tensorial order of the corresponding multipoles. In our experiment this prediction can be readily tested, since the individual resonances can be assigned to specific sublevel transitions by their resonance frequencies. The theoretical prediction is tested most easily for the resonance line at the origin of the frequency axis. It originates from the populations of the sublevels, which are invariant under rotation ($q = 0$). The data presented in Fig. 8 show clearly that the shape of this resonance line is virtually identical in the four experiments, in good agreement with the theoretical expectations.

The behavior of the line with $q = 2$ is also relatively simple to analyze: the line shape is inverted whenever the modulation phase is shifted by $\pi/2$. The corresponding multipole moments obviously have a periodicity of π. The resonance lines labeled $q = \pm 1$ change the line shape from approximately absorptionlike to dispersionlike when the modulation phase is shifted by $\pi/2$. The periodicity of this signal is 2π, as is expected for a first-order tensor

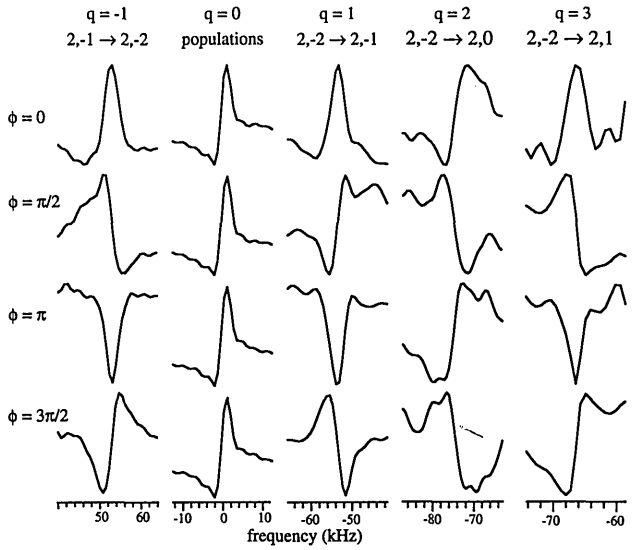

Fig. 8. Raman spectra of the Zeeman transitions in the sodium ground state recorded with various modulation phases during the first pulse. Each column represents one resonance line for four different phases. Above each column the assignment to the individual sublevel transitions is given as well as the order of the corresponding multipole moment.

element. The resonance line associated with the third-order tensor appears to have the same behavior as the $q = -1$ term. Theoretically we expect that a shift of the modulation phase by $\pi/2$ should change the phase of this resonance line by $3\pi/2$; however, such a phase shift is indistinguishable from the $-\pi/2$ phase shift observed for the $q = -1$ term. One must use rotation angles of less than $\pi/2$ to see the different behavior of these two signal components. In general, tensors of order q, q' can be distinguished if the rotation angle is smaller than $2\pi/(q - q')$.

The phase variation is analyzed more systematically in Fig. 9, where we have plotted the expected (straight lines) and the measured (squares, circles, and triangles) phases for a representative set of multipole components. Four different orientations of the atomic system were prepared by modulated optical pumping, and the phases of the resonance lines were measured. When necessary, we added multiples of 2π to the measured values to bring them from the range $[0, 2\pi]$ to the theoretically expected range $[2\pi n, 2\pi(n + 1)]$. The uncertainties in the measured data are highest for the weak resonance lines ($q = 2, 3$) but remain smaller than $\sim\pi/10$. The offset of the observed values, i.e., the phase at the reference orientation, is arbitrary and depends on various experimental parameters. The slope of the lines, however, demonstrates that the comparison of the signal phases for atomic states with different orientations indeed permits a determination of the tensorial order of the multipole components that cause these signal contributions.

The different response of the resonance lines to rotations of the atomic state can be used for the selective observation of particular tensor components. For this purpose we performed a sequence of experiments with different modulation phases $\phi = k\pi/2$ ($k = 0, 1, 2, 3$) and subsequently calculated linear combinations of the individual data sets. The necessary weighting coefficients c_{qk} depend on the order q of the tensor component that is to be observed: $c_{qk} = \exp(iqk\pi/2)$. The linear combinations are therefore equivalent to performing a Fourier transformation with respect to the rotation angle. This procedure separates the overall signal into components that transform irreducibly under the rotation.

Figure 10 shows the spectra that we obtained with this procedure: the top trace represents a spectrum obtained from a single experiment, including contributions from all possible multipole moments. We obtained the second trace by extracting the orientation-independent signal component by adding four spectra measured with phases shifted by $\pi/2$. The trace contains the signal components originating from $q = 0$ multipole components, i.e., the population differences, which are of course time independent. The signal components therefore appear at frequency $\omega = 0$. The $q = \pm 4$ components should also appear in this spectrum, since a rotation by multiples of $\pi/2$ leaves them in a state that is indistinguishable from its initial state. However, the intensity of these signal contributions is rather small, making their observation extremely difficult. The third trace contains the $q = 1$, -3 coherences; the strongest signals, which are due to $q = 1$ components, are those that can be observed in the normal Raman spectrum. The fourth trace contains the $q = \pm 2$ subspectrum with three transitions each from $q = +2, -2$. Comparison of the subspectrum with the $q = \pm 2$ transitions with the unedited spectrum at the top of the figure shows clearly that this separation of the subspectra makes it possible to observe weak resonance

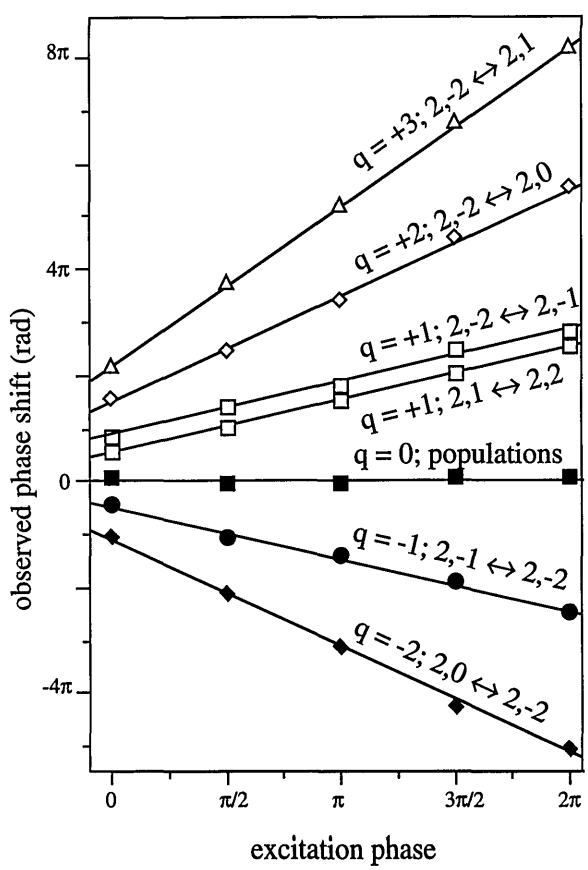

Fig. 9. Phase of the resonance lines as a function of the excitation phase. The solid lines represent the theoretical behavior; the circles, squares, and triangles show the experimental values.

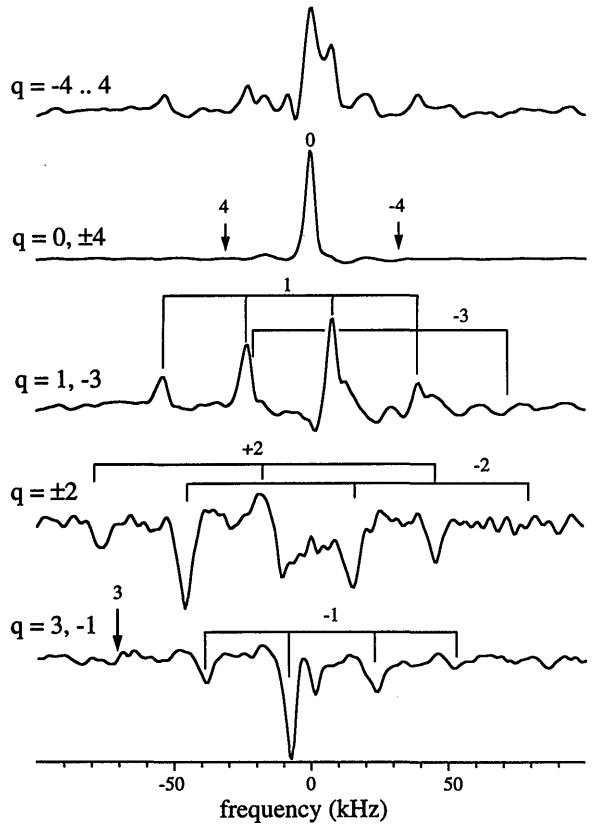

Fig. 10. Sublevel spectra for individual multipole orders obtained by linear combination of four spectra measured with the orientation of the atomic state rotated by 0, $\pi/2$, π, and $3\pi/2$. For details, see text.

$q = \pm 2$ lines that are just barely visible in the unedited spectrum.

5. CONCLUSION

The theoretical discussion as well as the experimental results presented here show that it is possible to measure the orientation of atomic multipole moments and to distinguish different multipole moments through their behavior under rotation. The phases that these multipole moments acquire during a rotation around the quantization axis are a measure of the tensorial order and can be observed in a sublevel spectrum. We have demonstrated the technique experimentally in atomic sodium; the multipole moments correspond to superpositions of different angular momentum substates of the electronic ground state. We excited these atomic multipole moments by modulated optical pumping in a transverse magnetic field. A rotation of the density operator around the direction of the magnetic field could then be achieved by a shift of the phase of the modulation. The different multipoles were monitored optically by use of laser-induced transfer of coherence between different multipole moments.

The different behavior of the various irreducible density-operator components can be used to introduce experimentally controllable selection rules to the experiment. We have demonstrated this possibility with the separation of subspectra by linear combination of data sets that were measured in systems with different orientations. Of course, this method is not limited to sodium or to electronic ground states but can also be applied to excited states. The potential for distinguishing signal contributions from different tensorial components of the density operator should be attractive primarily in cases in which the components are numerous and otherwise difficult to distinguish, such as in the case of severe spectral overlap, or for the observation of weak signals that are obscured by stronger signals from different multipole moments.

The method described here should be generally applicable to systems in which the Hamiltonian of the system has at least a uniaxial symmetry and rotations of the system around the symmetry axis are possible. If this minimum requirement of axial symmetry is not fulfilled, irreducible tensor operators lose their significance, and a classification according to their orders becomes meaningless. In cases of higher, e.g., spherical, symmetry of the Hamiltonian, it is also possible to use irreducible tensor operators as the basis operators and classify the resonances not only by the order q but also by the rank k of the tensor.[42]

ACKNOWLEDGMENTS

We thank Tilo Blasberg for experimental assistance and the Schweizerischer Nationalfonds for financial support.

REFERENCES

1. A. Omont, "Irreducible components of the density matrix. Application to optical pumping," Prog. Quantum Electron. **5,** 69–138 (1977).
2. G. Herman and A. Scharmann, "Untersuchungen zur Zeeman Spektroskopie mit Hilfe nichtlinearer Resonanzen eines multimoden Lasers," Z. Phys. **254,** 46–56 (1972).
3. M. Ducloy, M. P. Gorza, and B. Decomps, "Higher-order nonlinear effects in a gas laser: creation and detection of a hexadecupole moment in the neon $2p_4$ level," Opt. Commun. **8,** 21–25 (1973).
4. W. Gawlik, J. Kowalski, R. Neumann, and F. Träger, "Observation of the electric hexadecupole moment of free Na atoms in a forward scattering experiment," Opt. Commun. **12,** 400–404 (1974).
5. S. Giraud-Cotton, V. P. Kaftandjian, and L. Klein, "Magnetic optical activity in intense laser fields. I. Self-rotation and Verdet-constant," Phys. Rev. A **32,** 2211–2222 (1985).
6. K. H. Drake, W. Lange, and J. Mlynek, "Nonlinear Faraday and Voigt effect in a $J = 1$ to $J' = 0$ transition in atomic samarium vapour," Opt. Commun. **66,** 315–320 (1988).
7. L. M. Barkov, D. A. Melik-Pasheayev, and M. S. Zolotorev, "Nonlinear Faraday rotation in samarium vapor," Opt. Commun. **70,** 467–472 (1989).
8. R. Bernheim, *Optical pumping* (Benjamin, New York, 1965).
9. A Kastler, "Optical methods for studying Hertzian resonances," Science **158,** 214–221 (1967).
10. W. Happer, "Optical pumping," Rev. Mod. Phys. **44,** 169–249 (1972).
11. W. E. Bell and A. L. Bloom, "Optically driven spin precession," Phys. Rev. Lett. **6,** 280–281 (1961).
12. G. W. Series, "Theory of the modulation of light in optical pumping experiments," Proc. Phys. Soc. **88,** 957–968 (1966).
13. H. G. Dehmelt, "Modulation of a light beam by precessing absorbing atoms," Phys. Rev. **105,** 1924–1925 (1957).
14. R. B. Partridge and G. W. Series, "The modulated absorption of light in an optical pumping experiment on ^{4}He," Proc. Phys. Soc. **88,** 969–982 (1966).
15. W. Happer and B. S. Mathur, "Off-resonant light as a probe of optically pumped alkali vapors," Phys. Rev. Lett. **18,** 577–580 (1967).

16. S. Pancharatnam, "Modulated birefringence of a spin-assembly in magnetic resonance," Phys. Lett. **27A,** 509–510 (1968).
17. J. Mlynek, N. C. Wong, R. G. DeVoe, E. S. Kintzer, and R. G. Brewer, "Raman heterodyne detection of nuclear magnetic resonance," Phys. Rev. Lett. **50,** 993–996 (1983).
18. N. C. Wong, E. S. Kintzer, J. Mlynek, R. G. DeVoe, and R. G. Brewer, "Raman heterodyne detection of nuclear magnetic resonance," Phys. Rev. B **28,** 4993–5010 (1983).
19. P. Kulina and R. H. Rinkleff, "Determination of the tensor polarizabilities in Yb and Sm by quantum beat spectroscopy," Z. Phys. A **304,** 371–372 (1982).
20. A. P. Ghosh, C. D. Nabors, M. A. Attili, and J. E. Thomas, "$^3P_1$-orientation velocity-changing collision kernels studied by isolated multipole echoes," Phys. Rev. Lett. **54,** 1794–1797 (1985).
21. R. M. Lowe, D. S. Gough, R. J. McLean, and P. Hannaford, "Determination of ground-state depolarization rates by transmission Zeeman beat spectroscopy: application to Sm I $4f^6 6s^2\ ^7F_1$," Phys. Rev. A **36,** 5490–5493 (1987).
22. R. J. McLean, P. Hannaford, and R. M. Lowe, "Transmission Zeeman beat spectroscopy: application to the $7F$ ground level term of Sm I," Phys. Rev. A **42,** 6616–6628 (1990).
23. H. G. Dehmelt, "Slow spin relaxation of optically polarized sodium atoms," Phys. Rev. **105,** 1487–1489 (1957).
24. C. Cohen-Tannoudji, "Observation d'un déplacement de raie de résonance magnetique causé par l'exicitation optique," C. R. **252,** 394–396 (1961).
25. W. Lange and J. Mlynek, "Quantum beats in transmission by time-resolved polarization spectroscopy," Phys. Rev. Lett. **40,** 1373–1375 (1978).
26. T. Mishina, Y. Fukuda, and T. Hashi, "Optical generation and detection of $\Delta m = 2$ Zeeman coherence in the Cs ground state with a diode laser," Opt. Commun. **66,** 25–30 (1988).
27. S. Appelt, P. Scheufler, and M. Mehring, "Direct observation of single- and double-quantum sublevel coherence in rubidium vapor by optical Raman beat detection," Opt. Commun. **74,** 110–114 (1989).
28. C. Cohen-Tannoudji, "Theorie quantique du cycle de pompage optique," Ann. Phys. **7,** 423–460 (1962).
29. D. Suter and H. Klepel, "Indirect observation of 'forbidden' Raman transitions by laser-induced coherence transfer," Europhys. Lett. **19,** 469–474 (1992).
30. D. Suter, T. Marty, and H. Klepel. "Rotation properties of multipole moments in atomic sublevel spectroscopy," Opt. Lett. **18,** 531–533 (1993).
31. R. L. Shoemaker and R. G. Brewer, "Two-photon superradiance," Phys. Rev. Lett. **28,** 1430–1433 (1972).
32. D. Sutter, M. Rosatzin, and J. Mlynek, "Optically driven spin nutations in the ground state of atomic sodium," Phys. Rev. A **41,** 1634–1644 (1990).
33. D. Suter and T. Marty, "Laser induced dynamics of atomic sublevel coherences," Opt. Commun. **100,** 443–450 (1993).
34. J. Jeener, Lecture presented at the Ampére International Summer School II, Basko Polje, Yugoslavia, 1971 (Université Libre de Bruxelles, B-1050 Bruxelles, Belgium).
35. J. Jeener, B. H. Meier, P. Bachmann, and R. R. Ernst, "Investigation of exchange processes by two-dimensional NMR spectroscopy," J. Chem. Phys. **71,** 4546–4553 (1979).
36. R. R. Ernst, G. Bodenhausen, and A. Wokaun, *Principles of Nuclear Magnetic Resonance in One and Two Dimensions* (Oxford U. Press, Oxford, 1987).
37. D. Suter, H. Klepel, and J. Mlynek, "Time-resolved two-dimensional spectroscopy of optically driven atomic sublevel coherences," Phys. Rev. Lett. **67,** 2001–2004 (1991).
38. D. Suter and J. Mlynek, "Dynamics of atomic sublevel coherences during modulated optical pumping," Phys. Rev. A **43,** 6124–6134 (1991).
39. H. Klepel and D. Suter, "Transverse optical pumping with polarization-modulated light," Opt. Commun. **90,** 46–50 (1992).
40. M. Rosatzin, D. Suter, W. Lange, and J. Mlynek, "Phase and amplitude variations of optically induced spin transients," J. Opt. Soc. Am. B **7,** 1231–1238 (1990).
41. D. Suter and J. Mlynek, "Laser excitation and detection of magnetic resonance," in Adv. Magn. Opt. Reson. **16,** 1–83 (1991).
42. D. Suter and J. G. Pearson, "Experimental classification of multi-spin coherence under the full rotation group," Chem. Phys. Lett. **144,** 328–332 (1988).